Turkish J. Eng. Env. Sci.
34 (2010) , 189 – 199.

doi:10.3906/muh-1002-85

Geometrical effects of distributed attached mass on the natural frequency of thick cylindrical and spherical shells using higher-order theory

S. Mohammad Reza KHALILI, Shahab TAFAZOLI[1], Keramat MALEKZADEH[1], Ramesh Kumar MITTAL[2]
[1] *Centre of Excellence for Research in Advanced Materials and Structures, Faculty of Mechanical Engineering, K.N. Toosi University of Technology, Tehran-IRAN*
e-mail: smrkhalili2005@gmail.com
[2] *Department of Applied Mechanics, I.I.T, Delhi-INDIA*

Received 23.02.2010

Abstract

In this study, free vibrations of thick composite cylindrical and spherical shell panels with uniformly distributed attached masses were analyzed, using the standard Galerkin procedure. The stiffness effect of the distributed attached mass was taken into account for the first time, and the results were compared with well-known published results for which this effect was not considered. Various results for effects such as thickness, radii of curvature, and elasticity moduli are presented in this paper. Mass inertia of the distributed attached mass decreased the natural frequencies of the system, while the stiffness effect increased these values.

Key Words: Free vibrations, Laminated shell, Higher-order theory, Distributed attached mass

Introduction

In weight-sensitive engineering applications such as aerospace, and recently in transportation, fiber-reinforced materials are widely used, and their popularity continues to increase because of their high strength-to-weight and stiffness-to-weight ratios. As a result, the analyzing of laminated shells, especially thick ones, has increased in recent decades (Noor, 1973). The simplifying assumptions made in classical and first-order theories are reflected by the high percentage error in the results of thick composite and sandwich plates with stiff facings or distributed attached masses. Higher-order shell theories were introduced and developed by many researchers (Reddy, 1984; Garg et al., 2006). The use of higher-order shear deformation theory (HOST), which includes a realistic parabolic variation of transverse shear stress through the laminate thickness and warping of the transverse cross-section, is very important for the free vibration analysis of laminated composites, especially for thick composite and sandwich plates and shells with stiff faces or distributed attached mass. Khalili et al. (2008) investigated the free and forced vibration of multilayered composite cylindrical shells under transverse impulse load, as well as combined static axial loads and internal pressure. The procedure used in this analysis was first-order shear deformation theory, and the boundary conditions were considered to be simply support. The effects of fiber orientation, axial load, internal pressure, and some of the geometric parameters on the time response of the shells were determined. The results indicated that the dynamic responses were governed primarily by the natural period of the structure. More recently, Rahmani et al. (2009) introduced a free vibration analysis of composite sandwich cylindrical shells with flexible cores using a higher-order sandwich panel theory. The model consisted of a systematic approach for the analysis of sandwich shells with a flexible core, having high-order effects caused by the nonlinearity of the in-plane and the vertical displacements of the core. The behavior was presented in terms of internal resultants and displacements in the faces, peeling and shear stresses in the face-core interface, and stress and displacement fields in the core. Many publications on beams and rods with uniformly distributed mass (Chan et al., 1998) have been published, but only a limited amount of literature is available about plates with distributed masses. Gorman and Singal (1990) solved the free vibrations of a plate carrying a mass with a point-supported boundary by means of superposition. Rossi and Laura (1996) solved the vibration of a fully clamped plate with attached mass by combining the boundary element and finite element methods. Kopmaz and Telli (2002) investigated the free transversal vibrations of a plate carrying a distributed mass by means of a mathematical model. To discretize the derived partial differential equation, the Galerkin procedure was utilized. The eigenfrequencies and the eigenvectors of the system were then obtained. Wong (2002) analyzed the free bending vibration of a simply supported rectangular plate carrying a distributed mass loading with the Rayleigh-Ritz method. The effects of size and location of the mass loading on the changes of modal frequencies and shapes as demonstrated by the analysis of the numerical solution of the eigenvalue problem were investigated.

In this paper, for the first time, the natural frequencies of cylindrical and spherical shell panels were investigated using higher-order shell theory with an attached mass. The stiffness effect of the distributed attached mass was also investigated. Results with and without taking the stiffness into account were obtained and compared with each other. It was shown that by neglecting the stiffness, the error percentage in the behavior of the shell was increased.

Mathematical Model

Figure 1 shows a laminated composite curved shell with uniform thickness, carrying a distributed attached mass on its top surface. x, y, and z denote the orthogonal curvilinear coordinates where the x and y curves lie in the mid-surface of the laminate, and z is orthogonal to these 2 in order to make right-hand orthogonal coordinates. R_x and R_y represent the principal radius of the mid-surface curvature along the x- and y-axes. Neglecting the amount of z, comparing the radii of curvatures ($z/R = 0$), and using the constant radii of the curvatures, the shell used in this study is a doubly curved shell (Reddy, 2002).

In this study, a 12-variable displacement field (Garg et al., 2006) was used. By using this field, which demonstrates better kinematics compared to the first-order shear deformation and classical laminate theories, a shear correction factor may not be required. Expanding the displacements up to the cubic term in the thickness coordinate leads to the following equations:

$$\begin{cases} U\left(x,y,z,t\right) = u_0\left(x,y,t\right) + z\theta_x\left(x,y,t\right) + z^2 u_0^*\left(x,y,t\right) + z^3\theta_x^*\left(x,y,t\right) \\ V\left(x,y,z,t\right) = v_0\left(x,y,t\right) + z\theta_y\left(x,y,t\right) + z^2 v_0^*\left(x,y,t\right) + z^3\theta_y^*\left(x,y,t\right) \\ W\left(x,y,z,t\right) = w_0\left(x,y,t\right) + z\theta_z\left(x,y,t\right) + z^2 w_0^*\left(x,y,t\right) + z^3\theta_z^*\left(x,y,t\right) \end{cases} \tag{1}$$

where U, V, and W are the displacements of a general point in the laminate, and t is the time. u_o and v_o are the displacements related to the mid-surface, and w_o is the transverse displacement of a point on the mid-

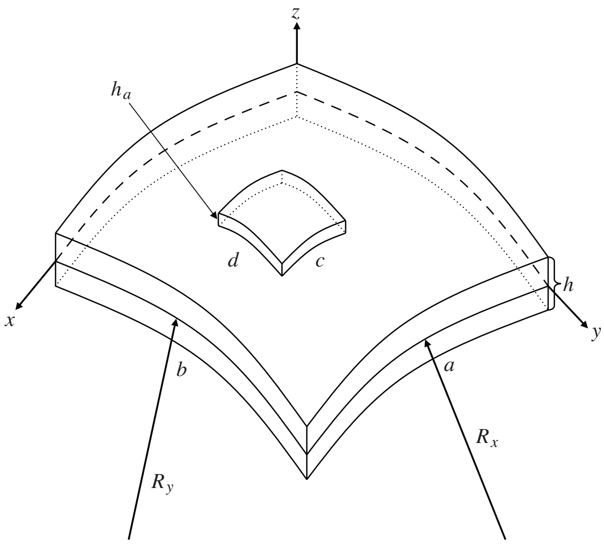

Figure 1. Laminated composite curved shell with uniform thickness and an attached mass.

surface. The terms θ_x, θ_y, θ_z, u_o^*, v_o^*, w_o^*, θ_x^*, θ_y^*, and θ_z^* are functions defined in the mid-surface. θ_x and θ_y are the rotations of the normal to the element middle plane about the x- and y-axes, and u_o^*, v_o^*, w_o^*, θ_x^*, θ_y^*, and θ_z^* are the higher-order terms in Taylor's series expansion and represent the higher-order transverse cross-sectional deformation modes. Linear normal and shear strains in an orthogonal curvilinear coordinate for a doubly curved shell (Reddy, 2004) were used. Hamilton's principal was used to define the equations of motion, with respect to the displacement field in Eq. (1). The analytical form is stated as follows (Reddy, 2002):

$$\int_0^t \delta L dt \equiv \int_0^t \left[\delta K - (\delta U - \delta V)\right] dt = 0 \tag{2}$$

where δK denotes the virtual kinetic energy, δU the virtual strain energy, and δV the virtual potential energy due to the applied loads. In order to add an attached mass, its virtual energy should be added to the main system. The main assumption is that this attached mass will take the form of the shell on the region in which it is located.

By means of Heaviside functions, the effect of the attached mass location will be satisfied (Kopmaz and Telli, 2002):

$$\begin{aligned} K_{\text{total}} &= K_{\text{shell}} + \mathrm{H}(x, y, x_0, y_0, c, d) K_{\text{attached mass}} \\ U_{\text{total}} &= U_{\text{shell}} + \mathrm{H}(x, y, x_0, y_0, c, d) U_{\text{attached mass}} \end{aligned} \tag{3}$$

where x_0 and y_0 are the coordinates of the corner of the attached mass, closest to the origin, and c and d are its width and length. H is a combination of Heaviside functions introduced by Kopmaz and Telli (2002). Integrating the resulting expression by part and collecting the coefficients of $\delta \mathrm{u}_0$, $\delta \mathrm{v}_0$, $\delta \mathrm{w}_0$, $\delta\theta_x$, $\delta\theta_y$, $\delta\theta_z$, $\delta \mathrm{u}_o^*$, $\delta \mathrm{v}_o^*$, $\delta \mathrm{w}_o^*$, $\delta\theta_x^*$, $\delta\theta_y^*$, and $\delta\theta_z^*$ results in the following equations:

$$
\begin{aligned}
&N_{xx,x} + N_{xy,y} + C_0 M_{xy,y} + \frac{Q_x}{R_x} + H\left(N_{xx,x} + N_{xy,y} + C_0 M_{xy,y} + \frac{Q_x}{R_x}\right)_a \\
&= I_0 \ddot{u}_0 + I_1 \ddot{\theta}_x + I_2 \ddot{u}_0^* + I_3 \ddot{\theta}_x^* + H\left(I_0 \ddot{u}_0 + I_1 \ddot{\theta}_x + I_2 \ddot{u}_0^* + I_3 \ddot{\theta}_x^*\right)_a \\
&N_{yy,y} + N_{xy,x} - C_0 M_{xy,x} + \frac{Q_y}{R_y} + H\left(N_{yy,y} + N_{xy,x} - C_0 M_{xy,x} + \frac{Q_y}{R_y}\right)_a \\
&= I_0 \ddot{v}_0 + I_1 \ddot{\theta}_y + I_2 \ddot{v}_0^* + I_3 \ddot{\theta}_y^* + H\left(I_0 \ddot{v}_0 + I_1 \ddot{\theta}_y + I_2 \ddot{v}_0^* + I_3 \ddot{\theta}_y^*\right)_a \\
&Q_{x,x} + Q_{y,y} - \tfrac{N_{yy}}{R_y} - \tfrac{N_{xx}}{R_x} + H\left(Q_{x,x} + Q_{y,y} - \tfrac{N_{yy}}{R_y} - \tfrac{N_{xx}}{R_x}\right)_a \\
&= I_0 \ddot{w}_0 + I_1 \ddot{\theta}_z + I_2 \ddot{w}_0^* + I_3 \ddot{\theta}_z^* + H\left(I_0 \ddot{w}_0 + I_1 \ddot{\theta}_z + I_2 \ddot{w}_0^* + I_3 \ddot{\theta}_z^*\right)_a \\
&M_{xx,x} + M_{xy,y} - Q_x + \tfrac{S_x}{R_x} + H\left(M_{xx,x} + M_{xy,y} - Q_x + \tfrac{S_x}{R_x}\right)_a \\
&= I_1 \ddot{u}_0 + I_2 \ddot{\theta}_x + I_3 \ddot{u}_0^* + I_4 \ddot{\theta}_x^* + H\left(I_1 \ddot{u}_0 + I_2 \ddot{\theta}_x + I_3 \ddot{u}_0^* + I_4 \ddot{\theta}_x^*\right)_a \\
&M_{yy,y} + M_{xy,x} - Q_y + \tfrac{S_y}{R_y} + H\left(M_{yy,y} + M_{xy,x} - Q_y + \tfrac{S_y}{R_y}\right)_a \\
&= I_1 \ddot{v}_0 + I_2 \ddot{\theta}_y + I_3 \ddot{v}_0^* + I_4 \ddot{\theta}_y^* + H\left(I_1 \ddot{v}_0 + I_2 \ddot{\theta}_y + I_3 \ddot{v}_0^* + I_4 \ddot{\theta}_y^*\right)_a \\
&S_{x,x} + S_{y,y} - N_{zz} - \tfrac{M_{xx}}{R_x} - \tfrac{M_{yy}}{R_y} + H\left(S_{x,x} + S_{y,y} - N_{zz} - \tfrac{M_{xx}}{R_x} - \tfrac{M_{yy}}{R_y}\right)_a \\
&= I_1 \ddot{w}_0 + I_2 \ddot{\theta}_z + I_3 \ddot{w}_0^* + I_4 \ddot{\theta}_z^* + H\left(I_1 \ddot{w}_0 + I_2 \ddot{\theta}_z + I_3 \ddot{w}_0^* + I_4 \ddot{\theta}_z^*\right)_a \\
&N_{xx,x}^* + N_{xy,y}^* + C_0 M_{xy,y}^* - 2S_x + \tfrac{Q_x^*}{R_x} + H\left(N_{xx,x}^* + N_{xy,y}^* + C_0 M_{xy,y}^* - 2S_x + \tfrac{Q_x^*}{R_x}\right)_a \\
&= I_2 \ddot{u}_0 + I_3 \ddot{\theta}_x + I_4 \ddot{u}_0^* + I_5 \ddot{\theta}_x^* + H\left(I_2 \ddot{u}_0 + I_3 \ddot{\theta}_x + I_4 \ddot{u}_0^* + I_5 \ddot{\theta}_x^*\right)_a \\
&N_{yy,y}^* + N_{xy,x}^* - C_0 M_{xy,x}^* - 2S_y + \tfrac{Q_y^*}{R_y} + H\left(N_{yy,y}^* + N_{xy,x}^* + C_0 M_{xy,x}^* - 2S_y + \tfrac{Q_y^*}{R_y}\right)_a \\
&= I_2 \ddot{v}_0 + I_3 \ddot{\theta}_y + I_4 \ddot{v}_0^* + I_5 \ddot{\theta}_y^* + H\left(I_2 \ddot{v}_0 + I_3 \ddot{\theta}_y + I_4 \ddot{v}_0^* + I_5 \ddot{\theta}_y^*\right)_a \\
&Q_{x,x}^* + Q_{y,y}^* - 2M_{zz} - \tfrac{N_{xx}^*}{R_x} - \tfrac{N_{yy}^*}{R_y} + H\left(Q_{x,x}^* + Q_{y,y}^* - 2M_{zz} - \tfrac{N_{xx}^*}{R_x} - \tfrac{N_{yy}^*}{R_y}\right)_a \\
&= I_2 \ddot{w}_0 + I_3 \ddot{\theta}_z + I_4 \ddot{w}_0^* + I_5 \ddot{\theta}_z^* + H\left(I_2 \ddot{w}_0 + I_3 \ddot{\theta}_z + I_4 \ddot{w}_0^* + I_5 \ddot{\theta}_z^*\right)_a \\
&M_{xx,x}^* + M_{xy,y}^* - 3Q_x^* + \tfrac{S_x^*}{R_x} + H\left(M_{xx,x}^* + M_{xy,y}^* - 3Q_x^* + \tfrac{S_x^*}{R_x}\right)_a \\
&= I_3 \ddot{u}_0 + I_4 \ddot{\theta}_x + I_5 \ddot{u}_0^* + I_6 \ddot{\theta}_x^* + H\left(I_3 \ddot{u}_0 + I_4 \ddot{\theta}_x + I_5 \ddot{u}_0^* + I_6 \ddot{\theta}_x^*\right)_a \\
&M_{yy,y}^* + M_{xy,x}^* - 3Q_y^* + \tfrac{S_y^*}{R_y} + H\left(M_{yy,y}^* + M_{xy,x}^* - 3Q_y^* + \tfrac{S_y^*}{R_y}\right)_a \\
&= I_3 \ddot{v}_0 + I_4 \ddot{\theta}_y + I_5 \ddot{v}_0^* + I_6 \ddot{\theta}_y^* + H\left(I_3 \ddot{v}_0 + I_4 \ddot{\theta}_y + I_5 \ddot{v}_0^* + I_6 \ddot{\theta}_y^*\right)_a
\end{aligned}
\tag{4}
$$

$$\begin{aligned}&S^*_{x,x}+S^*_{y,y}-3N^*_{zz}-\tfrac{M^*_{xx}}{R_x}-\tfrac{M^*_{yy}}{R_y}+H\left(S^*_{x,x}+S^*_{y,y}-3N^*_{zz}-\tfrac{M^*_{xx}}{R_x}-\tfrac{M^*_{yy}}{R_y}\right)_a\\&=I_3\ddot{w}_0+I_4\ddot{\theta}_z+I_5\ddot{w}^*_0+I_6\ddot{\theta}^*_z+H\left(I_3\ddot{w}_0+I_4\ddot{\theta}_z+I_5\ddot{w}^*_0+I_6\ddot{\theta}^*_z\right)_a\end{aligned} \quad \text{Cont.(4)}$$

in which:

$$(I_i)_a=\sum_{k=1}^{N}\int_{(z_a)_k}^{(z_a)_{k+1}}\bar{\rho}^{(k)}(z_a)^i dz_a \qquad (i=0,1,2,...,6)$$

$$I_i=\sum_{k=1}^{N}\int_{z_k}^{z_{k+1}}\rho^{(k)}(z)^i dz \qquad (i=0,1,2,...,6) \tag{5}$$

$$C_0=\frac{1}{2}\left(\frac{1}{R_x}-\frac{1}{R_y}\right).$$

Here, M, M^*, N, N^*, Q, Q^*, S, and S^* are the stress resultant components (Garg et al., 2006). The subscript "a" denotes the properties of the distributed attached mass. In the first expression of Eq. (5), which demonstrates the mass inertias of the distributed attached mass, it should be noted that the integral over z_a is measured from the mid-surface of the shell. Adding an attached mass leads the solution in such a way that the Navier solution will no longer be applicable. The solution used in this study is the Galerkin method. In order to solve the equations of motion, they must be transformed into the displacement coefficients.

The boundary condition for the simply supported shell is:

$$\begin{aligned}&v_0=w_0=\theta_y=\theta_z=v^*_o=w^*_o=\theta^*_y=\theta^*_z=N_x=N^*_x=M_x=M^*_x=0 \qquad \text{at} x=0 \text{ and } a,\\&u_0=w_0=\theta_x=\theta_z=u^*_o=w^*_o=\theta^*_x=\theta^*_z=N_y=N^*_y=M_y=M^*_y=0 \qquad \text{at} y=0 \text{ and } b.\end{aligned} \tag{6}$$

In order to satisfy these conditions, the double Fourier series was used as (Garg et al., 2006):

$$\begin{aligned}
u_0&=\sum_{m=1}^{\infty}\sum_{n=1}^{\infty}\{u_{0mn}\cos\alpha x\sin\beta y\}e^{i\omega t}, & v_0&=\sum_{m=1}^{\infty}\sum_{n=1}^{\infty}\{v_{0mn}\sin\alpha x\cos\beta y\}e^{i\omega t},\\
w_0&=\sum_{m=1}^{\infty}\sum_{n=1}^{\infty}\{w_{0mn}\sin\alpha x\sin\beta y\}e^{i\omega t}, & \theta_x&=\sum_{m=1}^{\infty}\sum_{n=1}^{\infty}\{\theta_{xmn}\cos\alpha x\sin\beta y\}e^{i\omega t},\\
\theta_y&=\sum_{m=1}^{\infty}\sum_{n=1}^{\infty}\{\theta_{ymn}\sin\alpha x\cos\beta y\}e^{i\omega t}, & \theta_z&=\sum_{m=1}^{\infty}\sum_{n=1}^{\infty}\{\theta_{zmn}\sin\alpha x\sin\beta y\}e^{i\omega t},\\
u^*_0&=\sum_{m=1}^{\infty}\sum_{n=1}^{\infty}\{u^*_{0mn}\cos\alpha x\sin\beta y\}e^{i\omega t}, & v^*_0&=\sum_{m=1}^{\infty}\sum_{n=1}^{\infty}\{v^*_{0mn}\sin\alpha x\cos\beta y\}e^{i\omega t},\\
w^*_0&=\sum_{m=1}^{\infty}\sum_{n=1}^{\infty}\{w^*_{0mn}\sin\alpha x\sin\beta y\}e^{i\omega t}, & \theta^*_x&=\sum_{m=1}^{\infty}\sum_{n=1}^{\infty}\{\theta^*_{xmn}\cos\alpha x\sin\beta y\}e^{i\omega t},\\
\theta^*_y&=\sum_{m=1}^{\infty}\sum_{n=1}^{\infty}\{\theta^*_{ymn}\sin\alpha x\cos\beta y\}e^{i\omega t}, & \theta^*_z&=\sum_{m=1}^{\infty}\sum_{n=1}^{\infty}\{\theta^*_{zmn}\sin\alpha x\sin\beta y\}e^{i\omega t}.
\end{aligned} \tag{7}$$

Here, $\alpha = \mathrm{m}\pi/\mathrm{a}$, $\beta = \mathrm{n}\pi/\mathrm{b}$, and ω is the natural frequency of the system. The next step was to apply these equations to the equations of motion in terms of displacement coefficients. After applying the equations, the shape functions had to be multiplied to their appropriate equations of motion, and then integrated over the surface of the shell. After integrating over the surface of the shell and collecting the coefficients, further relations in a matrix form resulted as follows:

$$\left\{[A] - \omega^2 [B]\right\}\{C\} = \{0\} \tag{8}$$

in which $\{C\}$ is the displacement vectors obtained by collecting the coefficients, which were sorted in an ascending order. $[A]$ is the stiffness matrix and $[B]$ is the mass matrix.

Results and Discussion

In order to solve the equations of motion, a program was set. After verifying the code by some well-known references in related fields, novel results for cylindrical and spherical panels carrying a distributed attached mass on its top were generated.

In the first example, free vibrations of cross-ply composite cylindrical and spherical panels were investigated, and the results were compared with the results of Reddy (2004). Material properties are shown in Table 1; the fundamental natural frequencies are listed in Table 2 for the cylindrical panel and Table 3 for the spherical panel.

Table 1. Material properties of composite shell panels (Reddy, 2004).

Elasticity Modulus	Shear Modulus	Lay-up	Dimensions	Poisson's ratio	Nondimensionalized Factor
$E1/E2 = 25$ $E2 = E3$	$G12 = G13 = 0.5E2$ $G23 = 0.2E2$	$(0°/90°)s$	$a = b$	$v12 = 0.25$	$\Omega = \omega a^2(\rho/E2)^{1/2}/\mathrm{h}$

Table 2. Nondimensional frequencies of simply supported symmetric cross-ply laminated composite cylindrical panel.

R/a	h/a	Reddy (2004)	Present Study
1	0.01	66.704	66.5594
	0.1	13.128	12.1839
5	0.01	20.361	20.343 8
	0.1	12.267	11.0538
Infinity	0.01	15.184	15.1381
(Plate)	0.1	12.226	11.7131

Table 3. Nondimensional frequencies of simply supported symmetric cross-ply laminated composite spherical panel.

R/a	h/a	Reddy (2004)	Present Study
1	0.01	126.33	126.299
	0.1	16.172	15.822
5	0.01	31.079	31.052
	0.1	12.437	11.934
Infinity	0.01	15.184	15.139
(Plate)	0.1	12.226	11.713

The maximum discrepancy in the case of a thin shell for the cylindrical panel was less than 0.2% with R/a = 1, and for the spherical panel it was also less than 0.02% for R/a = 1. In the case of thick shell panels, the maximum discrepancy for the spherical panel was less than 0.3%, and for the cylindrical panel it was less than 4%.

The second example for verification was that of an isotropic plate carrying a distributed attached mass at the center of the plate, without the stiffness effect. The reference that used here was a study by Kopmaz and Telli (2002). System properties are listed in Table 4. Results of 4 nondimensional frequencies for the plate without an attached mass are shown in Table 5, and for the plate with attached mass in Table 6.

Table 4. System properties of an isotropic plate carrying a distributed attached mass (Kopmaz and Telli, 2000).

Plate Properties	Attached Mass Properties	Nondimensionalized Factor
$b = 1.5a$ $a/h = 0.01$	$\rho aha = 10\rho h, ha = h, xo = 0.45a,$ $yo = 0.675a, c = 0.1a, d = 0.15a$	$\Omega = \omega(D/\rho a^4)^{-1/2}$

Table 5. Nondimensional frequencies of simply supported isotropic plate.

Present Study	Kopmaz and Telli (2002)
14.9618	14.2561
28.6130	27.4156
47.6247	43.8649
59.7813	57.0244

Table 6. Nondimensional frequencies of simply supported isotropic plate carrying a distributed attached mass.

Present Study	Kopmaz and Telli (2002)
12.6785	12.0092
28.3854	27.2403
47.2860	43.2103
59.7623	56.9853

In the Tables, a and b are the width and length of the plate, respectively; the subscript "a" represents the attached mass; ρ is the density of the plate and h is the thickness; x_0 and y_0 are the coordinates of the corner of the attached mass closest to the origin: c and d are the width and the length of the attached mass: and D is the flexural rigidity of the plate, which is defined as follows (Kopmaz and Telli, 2002):

$$D = \frac{Eh^3}{12(1 - v^2)} \tag{9}$$

where E and v are Young's modulus and Poisson's ratio of the plate, respectively.

The results of Kopmaz and Telli (2002) were based on classical plate theory, and the present theory was based on the higher-order shell theory. As can be seen, the results of the present theory are slightly higher than the results of Kopmaz and Telli (2002).

After validation of the model, 2 examples were set to demonstrate the effect of the distributed attached mass with stiffness effect. The first example pertained to the thickness and radii of the curvatures of the shell and the attached mass. The second demonstrated the effect of the elasticity moduli of the distributed attached mass. All results are available for the cylindrical and spherical panels. Properties of the shells are shown in Table 1. For the first example, the properties of the attached mass, which is located at the center of the panel, were set as follows:

$$E = E_1 \text{ (of panel)}, v = 0.33, c = 0.2a, d = 0.2a, \text{ and } \rho_a h_a = 10\rho h.$$

The first natural frequencies of the forgoing system are shown in Table 7 for the cylindrical panel and Table 8 for the spherical panel. In both Tables, the densities of the attached mass and the panel are assumed to be same. In these Tables, the first case is a shell without any attached mass; the second case is a shell with an attached mass, without including the stiffness effect; and the third case is a shell with an attached mass, including the stiffness effect. Quantities in parenthesis are the percentage of variation with respect to the first case. The following conclusions were derived from Tables 7 and 8. First, by fixing the amount of the first mass inertia term, which is the dominant term in the mass matrix, it becomes obvious from the results in the second case, in which the amount of variation percentage is constant, that the stiffness effect is shown by variation of the thickness and radii of curvatures. For instance, in Table 7, for the cylindrical composite panel, for R/a = 1 and h/a = 0.01, the effect of the attached mass when considering the stiffness effect (in the third case) is -15%; however, by increasing the radii of curvature until the panel became a plate, the effect was increased to

Table 7. Variation of first natural frequency of a cylindrical panel by thickness and radii of curvatures for three cases.

R/a	h/a	First Case*	Second Case**	Third Case***
1	0.01	66.4952	35.4515 (-%46)	56.3936 (-%15)
	0.02	35.1187	22.8217 (-%35)	32.9001 (-%6)
	0.05	17.8832	11.6563 (-%34)	21.2588 (+%18)
	0.07	14.7760	9.6463 (-%34)	18.8879 (+%27)
2	0.01	36.7391	23.4070 (-%36)	34.2017 (-%7)
	0.02	22.2195	14.1645 (-%36)	24.8571 (+%11)
	0.05	15.1135	9.6590 (-%36)	20.3454 (+%34)
	0.07	13.5506	8.6673 (-%36)	18.7880 (+%38)
5	0.01	20.2972	12.8678 (-%36)	24.0418 (+%18)
	0.02	16.3760	10.3790 (-%36)	21.9365 (+%33)
	0.05	14.1712	8.8200 (-%36)	20.0602 (+%41)
	0.07	13.1646	8.3623 (-%36)	18.7417 (+%41)
10	0.01	16.5826	10.4960 (-%36)	22.1896 (+%33)
	0.02	15.3375	9.7120 (-%36)	21.4797 (+%40)
	0.05	14.0287	8.8999 (-%36)	20.0136 (+%42)
	0.07	13.1076	8.3155 (-%36)	18.7274 (+%42)
20	0.01	15.5117	9.8158 (-%36)	21.7005 (+%39)
	0.02	15.0657	9.5378 (-%36)	21.3631 (+%41)
	0.05	13.9928	8.8742 (-%36)	19.9998 (+%42)
	0.07	13.0933	8.3027 (-%36)	18.7210 (+%42)
Plate	0.01	15.1375	9.5783 (-%36)	21.5345 (+%42)
	0.02	14.9739	9.4785 (-%36)	21.3250 (+%42)
	0.05	13.9807	8.8648 (-%36)	19.9922 (+%43)
	0.07	13.0885	8.2972 (-%36)	18.7138 (+%43)

*Shell without any attached mass

**Shell with attached mass, without including the stiffness effect

***Shell with attached mass, including the stiffness effect

+42%. Second, by increasing the thickness, the stiffness of the attached mass became more dominant on the first natural frequency. This parameter was affected by increasing or decreasing the radii of the curvature. This result is clear from Tables 7 and 8. In Table 8, for the spherical composite panel, for R/a = 1, the effect of the attached mass was increased from -19% to +7% by increasing the thickness ratio from 0.01 to 0.07. However, for the case of a plate, this variation was between 42% and 43%. Third, by increasing the radii of the curvatures, the stiffness effect was increased.

Table 8. Variation of first natural frequency of a spherical panel by thickness and radii of curvatures for three cases.

R/a	h/a	First Case*	Second Case**	Third Case***
1	0.01	126.2994	83.6955 (-%33)	102.0096 (-%19)
	0.02	64.0430	42.4651 (-%33)	55.0972 (-%14)
	0.05	27.6488	18.3677 (-%33)	27.4414 (%0)
	0.07	20.9347	13.9106 (-%33)	22.4831 (+%7)
2	0.01	68.2709	43.7462 (-%36)	57.4896 (-%15)
	0.02	36.2882	23.2675 (-%35)	33.8873 (-%6)
	0.05	18.8545	12.1193 (-%35)	22.2786 (+%18)
	0.07	15.6914	10.0932 (-%35)	19.8657 (+%26)
5	0.01	31.0516	19.6898 (-%36)	30.4635 (-%1)
	0.02	20.1352	12.7746 (-%36)	23.8397 (+%18)
	0.05	14.8992	9.4732 (-%36)	20.4124 (+%37)
	0.07	13.5543	8.6206 (-%36)	18.9494 (+%39)
10	0.01	20.3439	12.8798 (-%36)	24.0880 (+%18)
	0.02	16.4230	10.4050 (-%36)	21.9860 (+%33)
	0.05	14.2171	9.0228 (-%36)	20.0136 (+%40)
	0.07	13.2070	8.3823 (-%36)	18.7917 (+%42)
20	0.01	16.5948	10.5020 (-%36)	22.2020 (+%33)
	0.02	15.3499	9.7186 (-%36)	21.4933 (+%40)
	0.05	14.0403	8.9056 (-%36)	20.0288 (+%42)
	0.07	13.1183	8.3201 (-%36)	18.7427 (+%42)
Plate	0.01	15.1375	9.5783 (-%36)	21.5345 (+%42)
	0.02	14.9739	9.4785 (-%36)	21.3250 (+%42)
	0.05	13.9807	8.8648 (-%36)	19.9922 (+%43)
	0.07	13.0885	8.2972 (-%36)	18.7138 (+%43)

*Shell without any attached mass
**Shell with attached mass, without including the stiffness effect
***Shell with attached mass, including the stiffness effect

The second example is of the ratio of the elasticity moduli. Results are plotted in Figure 2 for the cylindrical and spherical panels. There, E_a is set equal to the E_1 of the panel, which was not small. As expected, by increasing this ratio, the stiffness of the system was increased, and the first natural frequency then also increased. This increase was almost linear, as is shown in Figure 2.

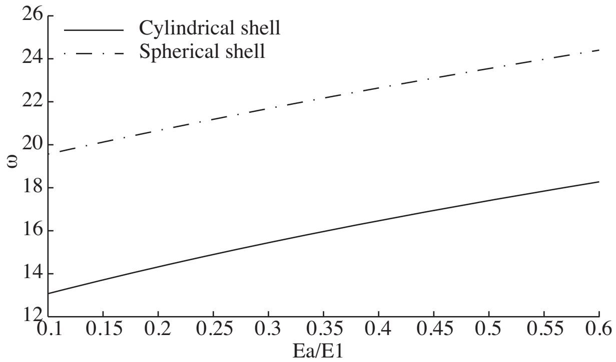

Figure 2. Variation of natural frequency by elasticity moduli for cylindrical and spherical panels.

Conclusion

In this paper, for the first time, the natural frequencies of cylindrical and spherical shell panels were investigated using higher-order shell theory with an attached mass. The stiffness effect of the distributed attached mass was also included in the analysis. The following conclusions were obtained:

- Natural frequencies of the system could be decreased by adding a distributed attached mass to the shell, and these variations could be very significant in some cases, when the stiffness of the patch was not included.
- By increasing the radii of the curvature, the effect of the stiffness of the attached mass on the natural frequency of the system was decreased.
- By increasing the thickness of the attached mass, the effect of the stiffness of the attached mass on the natural frequency of the system was increased.
- Elasticity modulus is a parameter that directly affects the stiffness of the attached mass and hence the stiffness of the whole system. By increasing the elasticity moduli of the attached mass, the effect of the stiffness of the attached mass on the natural frequency of the system was increased linearly.

References

Chan, K.T., Wang, X.Q. and Leung, T.P., “Free Vibration of Beams with Two Sections of Distributed Mass”, Journal of Vibration and Acoustics, 120, 944-948, 1998.

Garg, A.K., Khare, R.K. and Kant, T., “Higher-Order Closed-Form Solutions for Free Vibration of Laminated Composite and Sandwich Shells”, Journal of Sandwich Structures and Materials, 8, 205, 2006.

Gorman, D.J. and Singal, R.K., “Analytical and Experimental Study of Vibrating Rectangular Plates on Rigid Point Supports”, American Institute of Aeronautics and Astronautics, Inc., 1990.

Khalili, S.M.R., Azarafza, R. and Davar, A., “Transient Dynamic Response of Initially Stressed Composite Circular Cylindrical Shells under Radial Impulse Load”, Journal of Composite Structure, doi:10.1016/j.compstruct.2008.08.002, 2008.

Kopmaz, O. and Telli, S., “Free Vibration of a Rectangular Plate Carrying Distributed Mass”, Journal of Sound Vibration, 251, 39-57, 2002.

Noor, A.K., “Free Vibrations of Multilayered Composite Plates”, AIAA J., 11, 1038-1039, 1973.

Rahmani, O., Khalili, S.M.R. and Malekzadeh K., “Free Vibration Response of Composite Sandwich Cylindrical Shell with Flexible Core”, Journal of Composite Structure, doi:10.1016/j.compstruct.2009.10.021, 2009.

Reddy, J.N., “A Simple Higher-Order Theory for Laminated Composites”, ASME Journal of Applied Mechanics, 51, 745-752, 1984.

Reddy, J.N., “Energy Principles and Variational Methods in Applied Mechanics”, 2nd edition, John Wiley and Sons, 2002.

Reddy, J.N., “Mechanics of Laminated Composite Plates and Shells”, 2nd edition, CRC Press, 2004.

Rossi, R.E. and Laura, P.A.A., “Symmetric and Antisymmetric Normal Modes of a Cantilever Rectangular Plate: Effect of Poisson’s Ratio and a Concentrated Mass”, Journal of Sound and Vibration, 195, 142-148, 1996.

Wong, W.O., “The Effect of Distributed Mass Loading on Plate Vibration Behavior”, Journal of Sound and Vibration, 252, 577-583, 2002.